DMD Fast Forward. Published on April 21, 2008 as doi:10.1124/dmd.108.020917


DMD 20917

# Rate limiting steps in hepatic drug clearance: comparison of hepatocellular uptake and metabolism with microsomal metabolism of saquinavir, nelfinavir and ritonavir

Alison J. Parker and J. Brian Houston

School of Pharmacy and Pharmaceutical Sciences, University of Manchester

Running title: Hepatocellular uptake and drug metabolic clearance

Address for correspondence: Professor J B Houston

School of Pharmacy and Pharmaceutical Sciences

University of Manchester

Oxford Road

Manchester M13 9PT, UK

E-mail: brian.houston@manchester.ac.uk

Tables: 5

Figures: 6

References: 40

Number of words in Abstract: 222

Number of words in Introduction: 580

Number of words in Discussion: 1,491

Abbreviations used are:

ABT, aminobenzotriazole; BSA, bovine serum albumin; CLint, intrinsic clearance; fu, fraction of unbound drug; Kp, tissue-to-medium total drug concentration ratio; Kpu, tissue-to-medium unbound drug concentration ratio; OATP, organic avion transporter polypeptide; Perm, linear permeability parameter; PGP, p-glycoprotein; PI, protease inhibitor.

## Abstract

The intrinsic metabolic clearance of saquinavir, nelfinavir and ritonavir was determined over a range of concentrations (0.02 – 20 μM) in both rat liver microsomes and fresh isolated rat hepatocytes in suspension. Clearance values were found to be concentration dependent for both systems and at low concentrations microsomal clearance was much greater (7 to 14-fold) than in hepatocytes. Kinetic parameters showed substantially lower microsomal $K_m$ values (5-42 nM) compared to suspended rat hepatocytes (34-270 nM) but similar scaled $V_{max}$ values 2-26 nmol/min/g liver. In the absence of metabolism (achieved by pre-treating hepatocytes with a mechanism-based inhibitor of cytochrome P450), saquinavir, nelfinavir and ritonavir were actively and rapidly taken up into hepatocytes (cell:medium concentration ratios of 306-3352) and intracellular unbound drug concentrations between 5 and 12-fold higher than extracellular unbound concentrations were achieved. Comparison of the rate of uptake into hepatocytes with the rate of metabolism in hepatocytes and microsomes indicates that the former is the rate limiting step at low concentrations. The rate of metabolism saturates at lower concentrations (100 to 400-fold) than the rate of uptake, hence at higher concentrations metabolic rate-limited clearance occurs. In conclusion, the clearance of saquinavir, nelfinavir and ritonavir is extremely rapid and it is proposed that in the case of hepatocytes, and by inference in vivo, the rate of uptake limits the metabolic clearance of these three drugs.

## Introduction

In vitro systems are well established as valuable tools for studying various aspects of drug metabolism; in particular kinetic data obtained from in vitro systems can be scaled and used in the prediction of in vivo clearance (Houston and Carlile, 1997; Obach, 2001). Hepatic microsomes are at present the dominant in vitro system but have obvious disadvantages, such as the need for exogenously supplied cofactors and the lack of non-microsomal enzymes, in particular the phase II enzymes, and membrane transporter systems. As more drugs are being developed with non-cytochrome P450 dependant clearance, studies in hepatocytes are increasingly more important. Hepatocytes have traditionally been perceived as a complicated and time-consuming metabolizing system due to, in part, the need for fresh tissue for the cell isolation procedure. With recent advances in cryopreservation technologies the use of freshly isolated cells is no longer a necessity and hepatocytes can be stored at –80°C after isolation for a period of months, retain activity and provide useful human clearance prediction (Lau et al., 2002; McGinnity et al., 2004; Brown et al., 2007).

An obvious major advantage of hepatocytes is their intact structural integrity, which may result in intracellular drug concentrations that differ from those in the surrounding medium and are more representative of the in vivo situation. Several processes may contribute to this situation including intracellular binding (Hallifax and Houston, 2007) and membrane transporter activity (Lau et al., 2006). The study of transporter proteins expressed in hepatocytes has resulted in a substantial amount of literature including many comprehensive reviews (Mizuno et al., 2003; Shitara et al., 2006). It is becoming increasingly apparent that

the interplay between transporters and metabolism may have an impact on the absorption and clearance of drugs (Benet et al., 2004; Zamek-Gliszczyaski et al., 2006). For instance, an increase in the plasma levels of cerivastatin has been observed when co-administered with the immunosuppressant drug cyclosporin A (Muck et al., 1999). Shitara et al. (2003) confirmed cerivastatin is actively taken up into human hepatocytes and that cyclosporin A inhibited this uptake ($K_i$ values of 0.3-0.7 μM). Inhibition of cerivastatin metabolism by cyclosporin A gave only a small reduction in turnover, hence, suggesting that the interaction occurs via the inhibition of transporter mediated uptake and not via metabolic inhibition. A similar scenario may occur with repaglinade and gemfibrozil (Hinton et al., 2007). The inability to recognise these hepatic uptake and metabolic interplay phenomena may explain why for certain types of drugs in vivo clearance is not well predicted from simple hepatic microsomal studies (Lam and Benet, 2004). Human immunodeficiency virus protease inhibitors (Pls) are known to be substrates for hepatocyte uptake and efflux transporters (Kim et al., 1998; McRae et al., 2006) and are extensively and efficiently metabolized; thus they provide a good example for study of the interplay between transporter and metabolism.

The aims of this study were two-fold. First to delineate the kinetics and metabolism of saquinavir, nelfinavir and ritonavir in both isolated hepatocytes and hepatic microsomes. The source of these in vitro tissues was the rat to allow direct comparison of parameter values without the complication of intra-individual donor variability, which occurs with human preparations (Hallifax et al., 2005, Rawden et al., 2005). Secondly, to characterise the uptake of these three Pls in freshly isolated hepatocytes. Comparison of these data provides direct evidence that the clearance of saquinavir, nelfinavir and ritonavir in intact hepatocytes is extremely rapid in vitro and likely to be rate limited by their hepatic uptake in vivo.

## Materials and Methods

### Chemicals

Saquinavir, nelfinavir, [$^{14}$C] saquinavir and [$^{3}$H] nelfinavir were all gifts from Roche Products Ltd (Welwyn, U.K. and Basel, Switzerland) and ritonavir was a gift from Abbott laboratories (Illinois, U.S.A). [$^{3}$H] Ritonavir was purchased from Moravek Biochemicals Inc. (California, USA). All radiochemicals were >98% purity. Collagenase A and H were purchased from Roche Molecular Biochemicals, and silicone oil (AR20 and AR200) from Wacker Chemie GmbH. All other chemicals and reagents were purchased from Sigma Aldrich Company Ltd (Poole, UK), BDH Chemicals Ltd. (Lutterworth, Leicester, UK) or Fisher Scientific and were of the highest grade available. Uptake buffer contained sodium chloride, potassium chloride, potassium dihydrogen phosphate, magnesium chloride, sodium bicarbonate, D-glucose, HEPES and calcium chloride (all from Sigma).

### Preparation of Tissue

Hepatocytes were prepared using the collagenase perfusion method from Sprague Dawley male rats (200-250g) sacrificed by cervical dislocation according to the procedure described by Jones et al., (2005). Preparation of hepatocytes for uptake experiments was based on the same method using male Wistar rats anaesthetised with phenobarbital prior to hepatocyte isolation. Only cells with viability greater than 85% were used. Hepatic microsomes were prepared using the standard differential centrifugation method described by Jones et al., (2005) and were prepared from male Sprague Dawley rats.

**Incubation Methods**

Incubations were performed in Eppendorf tubes in a Thermomixer (Eppendorf AG, Hamburg, Germany) set at 37°C and 900 rpm and in a volume of 400 µl. The depletion of saquinavir, nelfinavir and ritonavir was measured over a range of concentrations (0.1 – 10, 0.1 – 10 and 0.01 - 2 µM for saquinavir, nelfinavir and ritonavir, respectively) with freshly isolated suspended rat hepatocytes (0.2 x $10^6$ cells/ml) or liver microsomes (0.2 mg protein/ml). Liver microsomes were diluted in phosphate buffer and a methanol solution of drug added (final solvent concentration of 1% v/v). After 5 minutes pre-incubation at 37°C 200 µl pre-warmed NADPH regenerating system was added to initiate reactions. Reactions were terminated by addition of 600 µl ice-cold acetonitrile containing an internal standard at the appropriate time point. Rat hepatocyte incubations were carried out in Williams medium E prewarmed to 37°C and reactions initiated by addition of 200 µl drug solution (in William medium E and 2% methanol) to 200 µl cell suspension (final solvent concentration of 1% v/v). Termination of reactions was by snap freezing in liquid nitrogen at the appropriate time point, 600 µl acetonitrile containing internal standard was added on thawing of the samples. All incubations were performed in duplicate.

Drug uptake into isolated hepatocytes was determined using the centrifugal filtration technique through a silicone oil layer (Hallifax and Houston, 2007). Following isolation, hepatocytes were re-suspended in uptake buffer (pH 7.4 and 37°C) containing 2 mM ABT (to prevent P450 mediated metabolism) and 2% BSA at 4 x $10^6$ cells/ml. Hepatocytes were dispensed into Eppendorf tubes and preincubated at 4°C or 37°C. The addition of saquinavir

(0.1 to 200 μM), nelfinavir or ritonavir (1 to 200 μM) in uptake buffer containing a fixed amount of the appropriate radiolabelled substrate and 2% BSA (final methanol concentration of 1%) initiated the uptake process. Aliquots were removed from the incubation at 6, 16, 26 and 36 seconds and dispensed into micro-tubes containing 10 μl 3M potassium hydroxide (lower layer) and 150 μl silicone oil (upper layer) and were immediately centrifuged for 30 seconds at high speed. After freezing in liquid nitrogen the KOH layer was removed using clippers and dropped into scintillation vials, which were then shaken overnight prior to analysis. Uptake rates at 4 and 37°C were determined by linear regression and expressed as pmol/sec. The rate at 4°C (passive uptake) was subtracted from 37°C rate (passive plus active) to determine temperature-dependant (active) uptake rate. Resultant active rates were plotted against drug concentration, corrected for binding to BSA in uptake buffer and kinetic parameters estimated.

The uptake of saquinavir, nelfinavir and ritonavir at 5 μM was also monitored over a longer time period to determine cellular drug concentration at equilibrium, in order to determine the cell to medium concentration ratio ($K_p$). Time points were taken at 6, 16, 26, 36, 70 and 120 seconds and a first order rate exponential input equation applied to the 37 minus the 4°C data.

**Measurement of Protein and Non-Specific Binding**

Protein binding was determined using Dianorm dialysis equipment (Diachema, Switzerland) and a dialysis membrane with a 5000 kD molecular weight cut-off. Drug solutions (1 μM) were prepared in each of the three incubation media containing protein (0.2 mg protein/ml liver microsomes, 0.02% BSA or 2% BSA) and 1 ml dialysed against protein-free media in a

water bath at 37°C for 4 hours. Samples were taken from each side of the chamber and fraction unbound (fu) was calculated by dividing the drug concentration in the dialysate by the drug concentration in the sample chamber. Non-specific binding was measured in hepatocyte and microsomal incubations with 1 μM saquinavir, nelfinavir or ritonavir where phosphate buffer replaced the NADPH regenerating system in microsomal incubations and 2 mM ABT was added to hepatocyte incubations to prevent metabolism. Aliquots were taken after 5 minutes and compared to known standards to calculate loss of compound due to non-specific binding. Previous experience has shown that the use of BSA in hepatocyte incubations is valuable in both minimising non-specific binding and stabilising the function of hepatocytes.

The extent of non-specific binding of saquinavir, nelfinavir and ritonavir to plastic and glass was also measured after the initial experiments indicated that back-calculated initial concentration was consistently lower than the nominal initial concentration. This was particularly noticeable in the hepatocyte metabolism incubations but was also detected in microsomal incubations. The degree of non-specific binding to plastic and glass varied between the drugs studied and the cumulative effect for these incubations is shown in Table 1. The greater effect seen in hepatocyte incubations is partly a consequence of the experimental design in which there is no protein present in the incubation until the addition of cells at zero time. The use of the observed initial drug concentration as opposed to the nominal initial concentration in all appropriate calculations corrected for this loss. This value was then corrected for fu in the incubation medium.

**Sample Preparation and Analysis**

Liver microsomes and hepatocytes samples were vortexed and centrifuged at 10,000g for 10 minutes. The supernatant was transferred to HPLC vials for analysis via LC-MS/MS.

Saquinavir together with verapamil (internal standard) were separated on a Luna C18 (2) 50 x 4.6 mm 3 µm column (Phenomenex) at 40°C using a binary gradient maintained at 1 ml/min by a Waters Alliance 2795 HT LC system. An initial mobile phase of 90% 0.001 M ammonium acetate/ 10% acetonitrile was ramped linearly to 82% acetonitrile/ 18% 0.001 M ammonium acetate (from minutes 1 to 4) following which the initial ratio was immediately re-established and equilibrated from minutes 4 to 5. The retention times were approximately 3.4 minutes (verapamil) and 3.5 minutes (saquinavir). Nelfinavir and its metabolite (M1) and ritonavir and its metabolites (M1, M2, M9 and M11) together with verapamil (internal standard) were separated using the same system as for saquinavir except that initial mobile phase of 90% 0.001 M ammonium acetate/ 10% acetonitrile was ramped linearly to 90% acetonitrile/ 10% 0.001 M ammonium acetate from minutes 1 to 4. The retention times were approximately 3.2 (verapamil), 3.3 (nelfinavir-M1), 3.4 minutes (nelfinavir), 3.9 (ritonavir-M11), 4.1 (ritonavir-M2 and ritonavir-M9) and 4.6 minutes (ritonavir and ritonavir-M1).

Saquinavir, nelfinavir and ritonavir and associated metabolites and internal standards were detected and quantified by atmospheric pressure electrospray ionisation MS/MS using a Micromass Quattro Ultima triple quadruple mass spectrometer. The LC column eluate was split and ¼ was delivered into the MS where the desolvation gas (nitrogen) flow rate was 600 l/hr, the cone gas (nitrogen) flow rate was 100 l/hr and the source temperature was 125°C.

Using positive ion mode, protonated molecular ions were formed using a capillary energy of 3.5 kV and cone energies of 38 V (saquinavir), 50 V (nelfinavir, nelfinavir-M1) and 60 V (verapamil, ritonavir, ritonavir-M1, ritonavir-M2, ritonavir-M9, ritonavir-M11). Product ions formed in argon at a pressure of $2x10^{-3}$ mbar and at varying collision energies were monitored as ion chromatograms which were subsequently integrated and quantified by quadratic regression of standard curves using Micromass QuanLynx 3.5 software.

**Data Processing**

For drug depletion studies, the log of drug concentration was plotted against time and the elimination rate constant calculated by fitting a single exponential decay. Initial drug concentration was corrected for protein binding prior to calculation of clearance. Metabolism data were also expressed as rates, representing a measure of substrate turnover per unit time per unit enzyme (as either microsomal protein or cell number), for each substrate concentration. This was achieved by multiplying the initial unbound concentration by clearance. These rate data were analysed by the Michaelis-Menten equation to determine by nonlinear regression the kinetic parameters $K_m$ and $V_{max}$. $CL_{int}$ and Perm were subsequently calculated by dividing $V_{max}$ by $K_m$ for the metabolic and transport data, respectively.

For the calculation of $K_p$ (total drug at equilibrium) at an initial concentration of 5 µM, two assumptions were made; firstly that drug concentration in adherent water was equivalent to medium concentration (correction for drug in adherent water was found to make minimal difference to calculated $K_p$) and secondly that the residual amount of drug (i.e. not detected in cells) represented drug in the medium. The unbound concentration of drug in the medium at

DMD Fast Forward. Published on April 21, 2008 as DOI: 10.1124/dmd.108.020917
This article has not been copyedited and formatted. The final version may differ from this version.



equilibrium ($C_{mu}$) was calculated using Equation 1 where $C_0$ is initial concentration of drug in media and $D_m$ is fraction of drug in media at equilibrium.

$$C_{mu} = D_m \times C_0 \times fu \quad (1)$$

The concentration of drug in cells at equilibrium ($C_c$) was calculated using Equation 2 where $A_e$ was the amount of drug in cells at equilibrium, $C_m$ the concentration of total drug in media at equilibrium, $V_a$ was the volume of the adherent water layer and $V_c$ was the intracellular volume.

$$C_c = \frac{A_e - (V_a \times C_m)}{V_c} \quad (2)$$

$K_p$ (total drug at equilibrium) was expressed as the ratio of $C_c$ to $C_{mu}$. Values for $V_a$ and $V_c$ were taken from Hallifax and Houston (2007). $K_{pu}$ (unbound drug at equilibrium) was calculated by dividing the initial uptake rate at 37°C (rate due to both transporters and passive permeability) by the initial uptake rate at 4°C (rate due to only passive permeability). The unbound intracellular fraction of drug was calculated by dividing $K_{pu}$ by $K_p$.

Data modelling was carried out using *Grafit* (version 4), Erithacus Software Ltd. and data are shown as mean values +/- standard deviation. Metabolism and uptake parameters from microsomal and hepatocyte incubations were calculated based on PI concentration corrected for both protein and non-specific binding, scaled and expressed as “per g liver” using the scaling factors 60 mg protein/g liver and 109 x $10^6$cells/g liver (Houston and Carlile, 1997).

## Results

### Non-specific and Protein Binding Characteristics

The extent of binding at the drug concentrations used within the hepatocyte metabolism (0.02% BSA), microsomal (0.2 mg/ml) and hepatocyte uptake (2% BSA) incubation matrices generally increased with the protein content. However the rank order in terms of fu for the three drugs differed between the three matrices: for example ritonavir>saquinavir>nelfinavir in microsomes compared with saquinavir>ritonavir>nelfinavir in hepatocyte uptake buffer (Table 1). Substantial binding (90% or more) was evident within the hepatocyte uptake and microsomal incubates for nelfinavir. Saquinavir and ritonavir fu were similar in both matrices, fu were approximately 0.3 and 0.5, respectively, but nelfinavir demonstrated a much greater affinity for microsomal protein, fu = 0.1 in 0.2 mg protein/ml for liver microsomes compared with 0.5 in 0.02% BSA. All parameters refer to unbound drug concentrations as they are corrected for both protein and non-specific (plastic and glass, see Methods) binding.

### Drug Depletion Studies

The depletion of saquinavir, nelfinavir and ritonavir was measured over a range of concentrations (0.1 – 10, 0.1 – 10 and 0.01 - 2 μM for saquinavir, nelfinavir and ritonavir, respectively) in freshly isolated suspended rat hepatocytes (0.2 x $10^6$ cells/ml) and microsomes (0.2 mg protein/ml). All depletion profiles appeared log-linear over the time course studied (up to a maximum of 20 min) and involved a minimum of 15% parent drug loss.

Expression of data in terms of the metabolic rate at each concentration (corrected for fu in incubation) for saquinavir is shown in Figure 1 (panels A and B). Saquinavir metabolism followed Michaelis-Menten kinetics in microsomes and hepatocytes and the kinetic parameters $V_{max}$, $K_m$ and $Cl_{int}$ are listed in Tables 2 and 3 for these two *in vitro* systems, respectively. The data were also expressed as Clearance plots, as shown for saquinavir in Figure 1 (panels C and D). Clearance in suspended hepatocytes approached concentration-independence (representing $Cl_{int}$) at concentrations below 0.02 µM, illustrated by the plateau at low saquinavir concentration. Above 0.02 µM, clearance became saturated as illustrated by the progressive decline in saquinavir clearance with respect to increasing saquinavir concentration. In microsomes due to the apparently low Km, $Cl_{int}$ could only be estimated by back extrapolation as very rapid turnover and analytical sensitivity prevented determination below of initial unbound drug concentration of 0.03 µM.

Clearance plots for nelfinavir and ritonavir are shown in Figures 2 and 3, respectively for both the hepatocytes and microsomal incubations. As in the case of saquinavir the turnover of these two Pls was substantially faster in microsomes than in hepatocytes. Michaelis-Menten kinetic behaviour was observed in hepatocytes for both drugs and the $K_m$ and $V_{max}$ values are listed in Table 2. In microsomes again there is the issue of lack of experimental data at very low substrate concentrations, below 0.008 µM and 0.003 µM for nelfinavir and ritonavir respectively. Also there was some suggestion of substrate inhibition for nelfinavir, demonstrated by a slight decrease in metabolic rate at high nelfinavir concentrations (>0.5 µM). Thus, in addition to the Michaelis-Menten equation, a substrate inhibition equation was also applied to the nelfinavir microsomal data however only minor changes were evident (see Table 3). The kinetic parameters obtained in both in vitro systems (Tables 2 and 3) represent

the sum of more than one pathway as saquinavir, ritonavir and nelfinavir form multiple metabolites.

**Metabolite Formation Studies**

In addition to measuring the time course of depletion of parent drug, metabolite appearance was also investigated for ritonavir and nelfinavir.

Four ritonavir metabolites were identified in hepatocyte incubations and were quantified in arbitrary units as metabolite standards were not available. The metabolites M1 (loss of the thiazolyl carbamate moiety), M2 (oxidation at the terminal isopropyl group), M9 (oxidation on the methylthiozolyl moiety) and M11 (loss of the isopropylthiazolylmethyl moiety) were detected; previously identified by Denissen et al. (1997). The Michaelis-Menten kinetic equation was applied to the formation of all four metabolites (Figure 4A) and the $K_m$ values for the individual metabolites were 0.034 ± 0.015, 0.13 ± 0.055, 0.029 ± 0.014 and 0.024 ± 0.014 μM for M1, M2, M9 and M11, respectively. Assuming approximately equal mass spectrometry sensitivities a rank order of $Cl_{int}$ can be made by dividing the $V_{max}$ (in arbitrary units) by $K_m$. The highest $Cl_{int}$ was observed with M1, the $Cl_{int}$ of M2, M9 and M11 were all approximately half that of M1.

Four metabolites M1, M2, M9 and M11 were also detected in microsomal incubations containing ritonavir and again Michaelis-Menten kinetics were observed in each case (Figure 4B). The $K_m$ values for the individual metabolites were 0.028 ± 0.005, 0.091 ± 0.021, 0.015 ± 0.007 and 0.029 ± 0.019 μM for M1, M2, M9 and M11, respectively. The rank order of $Cl_{int}$ for the four metabolites, calculated using the $V_{max}$ values (in arbitrary units) and assuming equal mass spectrometry sensitivity, was M1>M2=M9>M11.

Two metabolites of nelfinavir were detected after incubating with rat hepatocytes, previously identified as M1 (3'methoxy-4'hydroxynelfinavir) and M8 (nelfinavir hydroxy-*t*-butamide) by Zhang et al. (2001). Only M1 was quantifiable and its rate of formation was consistent with Michaelis-Menten kinetics with a $K_m$ of 2.3 ± 1.2 μM.

M1 and M8 were also identified in microsomes, but only M1 was quantifiable. An increase in initial rate of formation with increasing nelfinavir concentration was observed up to 5 μM, but the rate at 10 μM was slower than that at 5 μM indicating possible substrate inhibition. Both substrate inhibition and Michaelis-Menten kinetic fits were applied and $K_m$ values for the formation of M1 were 0.027 μM (Michaelis-Menten fit) and 0.08 μM (substrate inhibition fit).

There was excellent agreement between the $K_m$ values for ritonavir M1 formation and parent drug depletion in hepatocytes. However, $K_m$ values were consistently higher than parent drug depletion for the specific metabolites of ritonavir in microsomes and nelfinavir in both systems. This observation highlights the hybrid nature of the kinetic parameters obtained by drug depletion. However the much faster turnover of both ritonavir and nelfinavir, evident in the drug depletion studies, was confirmed from the metabolite formation studies.

**Hepatocyte Uptake Studies**

Initial uptake rates of saquinavir, nelfinavir and ritonavir into rat hepatocytes were assessed between 0.1 and 200 μM at both 37 and 4ºC (Figure 5A-C). Significant temperature-dependant uptake of saquinavir, nelfinavir and ritonavir was observed indicative of cell

uptake via an active process. For saquinavir, saturation of uptake was not observed at unbound drug concentrations below 28 μM therefore kinetic parameters were limited to the calculation of the linear permeability term. For nelfinavir and ritonavir, saturation of uptake was observed at high concentrations (see Figure 5B and C), and the Michaelis-Menten equation was applied. The resultant kinetic parameters and Perm (estimated by dividing $V_{max}$ by $K_m$), values for saquinavir, nelfinavir and ritonavir are shown in Table 2. It can be seen that all transporter parameters were substantially higher than the corresponding metabolic parameters.

Figure 5D shows uptake time profiles for active uptake into hepatocytes for saquinavir, nelfinavir and ritonavir, obtained by substracting the 4°C rate from the rate at 37°C. The rate constants for the first order uptake obtained from the exponential time profile were 0.022, 0.047 and 0.0504 $sec^{-1}$ for saquinavir, nelfinavir and ritonavir, respectively and the rank order of these measures of permeability were consistent with those obtained in the initial rate experiments (Table 2). Comparison of the plateau values of these curves indicates that nelfinavir showed the highest extent of intracellular accumulation and saquinavir and ritonavir accumulation were substantially lower. From the cell and medium drug concentrations at plateau, $K_p$ values for saquinavir, nelfinavir and ritonavir were calculated and showed a 10-fold range (Table 4).

In order to resolve the $K_p$ values into transporter and intracellular binding components, $K_{pu}$ values were calculated to obtain a pure measure of the former component. Similar $K_{pu}$ values were found for the three drugs (within a 2-fold range) and constituted a minor

component of the overall $K_p$ (<2%). The rank order of intracellular binding (as reflected in the unbound values in Table 4) was saquinavir=ritonavir>>nelfinavir. The intracellular unbound fractions for ritonavir and saquinavir are similar as both the $K_p$ and the $K_{pu}$ show a 2-fold difference.

**Comparison of hepatocellular uptake and metabolism with microsomal metabolism**

In order to allow direct comparison between the microsomal and hepatocyte derived kinetic parameters, rates and clearances were expressed per g of intact liver by the use of scaling factors. Figure 6 illustrates the scaled data for uptake and metabolism. At low substrate concentrations microsomal values markedly exceed hepatocyte metabolism, whereas the latter are in close agreement with the hepatocyte uptake values. In Table 5 the corresponding linear parameters for clearance and permeability in hepatocytes and microsomes are expressed in terms of units of liver to allow direct comparison of the in vitro systems.

**Discussion**

Pls are a class of drugs known to be extensively and rapidly metabolised in vivo and to be substrates for several transporter proteins (Kashuba, 2005; McNicholl, 2004). We have investigated the metabolism of saquinavir, nelfinavir and ritonavir in liver microsomes and in suspended hepatocytes to elucidate hepatic clearance mechanisms, in order to allow rational prediction of *in vivo* clearance. Both substrate depletion and metabolite formation approaches were used. Pls generally are highly plasma protein bound due to their high lipophilicity therefore binding to protein present in *in vitro* incubation matrices was measured. Saquinavir, nelfinavir and ritonavir all showed significant non-specific binding, which was corrected for throughout this study to provide true kinetic parameters. Nelfinavir has previously been shown to exhibit a higher degree of intracellular accumulation compared with other Pls (Khoo et al., 2002; Jones et al., 2001).

Significantly higher metabolic rates (corresponding to lower $K_m$ values) in rat liver microsomes were observed when the kinetics of saquinavir, nelfinavir and ritonavir in rat liver microsomes were compared to suspended rat hepatocytes; ranging from 6-fold lower for ritonavir and saquinavir to 30-fold lower for nelfinavir. When nelfinavir metabolite data are compared a similar picture is observed where the $K_m$ for nelfinavir metabolite M1 in rat microsomes was 80-fold lower than the $K_m$ in suspended rat hepatocytes. The differences between ritonavir metabolite $K_m$ values in rat microsomes and hepatocytes were less. $V_{max}$ values for rat microsomes and suspended rat hepatocytes, when scaled to common units of liver weight were relatively similar; ranging from 3.2 and 2.4 for ritonavir to 26 and 13 nmol/min/g liver for saquinavir for rat microsomal and rat hepatocytes, respectively. It could be argued that the nelfinavir $V_{max}$ in microsomes (6 nmol/min/g liver) was underestimated

due to either non-log-linear depletion or substrate inhibition whereas in suspended hepatocytes (25 nmol/min/g liver) there was no evidence of substrate inhibition, possibly due to the presence of phase II enzymes preventing a build up of competing metabolite(s) (Jones et al., 2005).

To date there is minimal literature information on in vitro metabolism of saquinavir, nelfinavir and ritonavir in rat liver microsomes and information in rat hepatocytes would appear to be non-existent. Yamaji et al. (1999) studied kinetics in Wistar rat liver microsomes of a number of Pls and observed $K_m$ values of 8.3 and 5.9 μM and $V_{max}$ values of 1.4 and 0.7 nmol/min/mg protein for saquinavir and nelfinavir, respectively. Shibata et al. (2002b) studied saquinavir metabolism also in Wistar rat liver microsomes and determined $K_m$ and $V_{max}$ values of 37 μM and 4700 nmol/min/mg protein. These parameters differ from those determined in this work. They also differ from each other and this affords very different estimates of saquinavir $Cl_{int}$: 0.17, 126 and 11 μl/min/mg protein for Yamaji et al., Shibata et al. and this work, respectively. Discrepancies in parameter estimates may result from differences in methodology, although all 3 studies estimated kinetics by determining depletion of parent drug together with the lack of correction for protein and non-specific binding leading to significantly higher $K_m$ estimates. No literature was identified on *in vitro* metabolism of ritonavir in rat hepatocytes but *in vivo* and microsomal data published by Denissen et al. (1997) and Kumar et al. (1996) determined that metabolites M1, M2, M9 and M11 were the predominant primary metabolites, which agrees with observations in our work. Studies have been carried out in human liver microsomes at comparable substrate concentrations to the present study and low $K_m$ estimates reported: 0.61 and, 0.92 μM for saquinavir (Ealing et al., 2002) and ritonavir (Koudriakova et al., 1998)..

Comparison of saquinavir scaled $Cl_{int}$ ($V_{max}/K_m$) (Table 5) mainly reflects the disparity in $K_m$ values; saquinavir rat liver microsomes $Cl_{int}$ is over 12 times higher than $Cl_{int}$ in suspended rat hepatocytes. A comparison of nelfinavir scaled $Cl_{int}$ shows that rat liver microsomes $Cl_{int}$ is between 5 and 8 times higher than $Cl_{int}$ in suspended rat hepatocytes depending on whether a Michaelis-Menten or substrate inhibition fit was applied. Ritonavir scaled $Cl_{int}$ value in rat liver microsomes is 9 times higher than $Cl_{int}$ in suspended rat hepatocytes, again mainly due to the difference in $K_m$. Consideration of figures 1-3 not only highlight the very rapid turnover in microsomes with respect to hepatocytes but also the issue of the lack of experimental data at the lower substrate concentrations thus the $K_m$ value and intrinsic clearance values are obtained by back extrapolating the higher concentration data as part of the nonlinear regression process. However, the difference between the hepatocyte and microsomal kinetic parameters are entirely consistent with the metabolic rate data shown in these figures.

The higher $K_m$ values observed in rat hepatocytes suggest that the unbound intracellular concentrations of saquinavir, nelfinavir and ritonavir differ from the unbound extracellular concentration. It would seem reasonable to assume that the microsomal $Cl_{int}$ represents the 'true' $Cl_{int}$, with no non-metabolic limitations and unbound drug concentration in the microsomal incubation being equivalent to the unbound drug concentration available to the drug-metabolising enzymes. Whereas for hepatocyte $Cl_{int}$, determination of the intracellular free drug concentration available to the enzyme is unknown. Various factors will affect the free intracellular drug concentration including influx of drug into the cell (via active and passive means), efflux out of the cell, and intracellular protein binding. These results may result in a different $K_m$ value in hepatocytes.

Saquinavir, nelfinavir and ritonavir all showed temperature-dependant uptake into suspended rat hepatocytes and kinetic parameters were calculated for nelfinavir and ritonavir (saquinavir uptake showed no saturation over the concentration range studied). The $K_m$ values for nelfinavir and ritonavir were similar whilst $V_{max}$ differed by 4-fold. Permeability values estimated from the ratio of $V_{max}$ to $K_m$ (nelfinavir and ritonavir) or from the slope of the rate plot (saquinavir) gave a rank order of permeability of nelfinavir>ritonavir>saquinavir (Table 2), comparable to the rank order of permeability determined by measuring uptake rate to equilibrium (Figure 5D). Saquinavir, nelfinavir and ritonavir all demonstrate high $K_p$ values (310-3350) with the nelfinavir $K_p$ significantly higher than the others. In contrast $K_{pu}$ was found to be similar for the three drugs (6-11, see Table 4) indicating a similar dependence on transporters. Intracellular fraction unbound values for all three drugs were low, particularly for nelfinavir where 99.8% of intracellular nelfinavir was estimated to be bound. In contrast, high $K_p$ values (100-1300) have also been measured for lipophilic amines such as propranolol and fluoxetine, however, once $K_p$ is corrected for intracellular binding there is essentially no evidence for active uptake (Hallifax and Houston, 2007).

Comparison of Perm and $Cl_{int}$ values measured in rat hepatocytes (Table 2) reveals the same rank order across the three drugs and a similar order of magnitude between the parameters for each drug. Interestingly, hepatocyte metabolic parameters are consistently lower than microsomal $Cl_{int}$ for all three compounds indicating that uptake into cells, rather than enzyme factors, govern hepatocellular clearance. At low saquinavir concentrations, the metabolic rate in rat microsomes is greater than uptake rate in rat hepatocytes, reflecting uptake limitation of metabolism in rat hepatocytes. In contrast, at higher concentrations once metabolic clearance becomes saturated, the metabolic rate is no longer limited by uptake. This is illustrated in

Figure 6 saquinavir, ritonavir and nelfinavir. Although the transport and metabolic studies were carried out using different rat strains, we feel this does not compromise the interpretation of these data. However, as rat strain differences in transporters have yet to be investigated this remains a moot point.

*In vivo*, hepatocytes express both efflux and uptake transporters and it is important to consider that the apparent uptake rate may be affected by efflux rate especially as Pls are well documented to be substrates for efflux transporters (Srinivas et al., 1998). An increase in uptake rate in cell lines expressing both PGP and uptake transporters has been observed using PGP inhibitors (Jones et al., 2001; Su et al., 2004). In freshly isolated rat hepatocytes expression of efflux transporters may be significantly lower than *in vivo* due to down regulation and internalisation of the apical membrane and although PGP has been detected on the hepatocyte apical membrane after isolation using immunohistochemical techniques, it is at a lower abundance than *in vivo* (Bow et al., 2008). Lam et al., (2006) have observed changes in uptake and clearance of erythromycin in rat hepatocytes following treatment with rifampin and GF120918 consistent with decreased and increased transporter activity (OATPs and PGP) respectively.

Although there is little published work on uptake of PIs in the rat, some studies have been carried out in various human systems. Saquinavir, nelfinavir and ritonavir have all been shown to inhibit uptake of the OATP substrates estradiol 17β-glucuronide (Tirona et al., 2003) and fexofenadine (Dresser et al., 2002), suggesting they may possibly be substrates. Saquinavir has also been confirmed to be a substrate for OATP-A (OATP 1A2/*SLC21A3*) in

HepG2 cells and *Xenopus* oocytes, $K_m$ values determined were 94.6 and 36.4 μM, respectively (Su et al., 2004) which is consistent with this work where a $K_m$ of >28 μM was estimated.

In the rat all three PIs studied are high clearance drugs (Gao et al., 2002; Shibata et al., 2002b; Lin, 1997). Using the well-stirred liver model, hepatic extraction ratios were predicted from microsomal and hepatocellular $Cl_{int}$ and Perm values, and as shown in Table 5 high extraction ratios were obtained in all cases. Thus it is difficult at this level of comparison to conclude which in vitro system provides the most accurate prediction. However it is clear from the above discussion that microsomal $Cl_{int}$ values are misleading in terms of the magnitude of the turnover of these PIs in vivo. Thus while cellular uptake rate limits the metabolism of saquinavir, nelfinavir and ritonavir within intact hepatocytes, this process is efficient and strongly indicates that the hepatic clearances for these PIs are all blood flow limited in the in vivo situation.

**ACKNOWLEDGEMENTS**

We are grateful to Dr Nadine Warner (Roche Products Ltd, Welwyn Garden City, UK) for initiating this BBRSC CASE project and Dr Christoph Funk (Hoffman-La Roche Ltd, Basel, Switzerland) for valuable assistance and laboratory facilities for the hepatocyte uptake studies.

**References**

Benet ZL, Cummins CL and Wu CY (2004) Unmasking the dynamic interplay between efflux transporters and metabolic enzymes. *Int J Pharmac* **277**: 3-9.

Bow DAJ, Perry JL, Miller DS, Pritchard JB and Brouwer KLR (2008) Localization of P-gp (Abcb1) and Mrp2 (Abcc2) in freshly isolated rat hepatocytes. *Drug Metab Dispos* **36**:198-202.

Brown HS, Griffin M and Houston JB (2007) Evaluation of cryopreserved human hepatocytes as an alternative in vitro system to microsomes for the prediction of metabolic clearance. *Drug Metab Dispos* **35**: 293-301.

Denissen JF, Grabowski BA, Johnson MK, Buko AM, Kempf DJ, Thomas SB and Surber BW (1997) Metabolism and disposition of the HIV-1 protease inhibitor ritonavir (ABT-538) in rats, dogs, and humans. *Drug Metab Dispos* **25**:489-501

Dresser GK, Bailey DG, Leake B, Schwarz UI, Dawson PA, Freeman DJ and Kim RB (2002) Fruit juices inhibit organic anion transporting polypeptide-mediated drug uptake to decrease the oral bioavailability of fexofenadine. *Clin Pharmacol Ther* **71**:11-20.

Eagling VA, Wiltshire H, Whitcombe IWA and Back DJ (2002) CYP3A4-mediated hepatic microsomes of the HIV-1 protease inhibitor saquinavir in vitro *Xenobiotica* **32**:1-17

Gao W, Kishida T, Kageyama M, Kimura K, Yoshikawa Y, Shibata N and Takada K (2002) Hepatic and intestinal contributions to pharmacokinetic interaction of indinavir with amprenavir, nelfinavir and saquinavir in rats. *Antivir Chem Chemother* **13**:17-26.

Hallifax D, Rawden HC, Hakooz N and Houston JB (2005) Prediction of metabolic clearance using cryopreserved human hepatocytes: kinetic characteristics for five benzodiazepines. *Drug Metab Dispos* **33**: 1852-1858.

Hallifax D and Houston JB (2007) Saturable uptake of lipophilic amine drugs into isolated hepatocytes: Mechanisms and consequences for quantitative clearance prediction. *Drug Metab Dispos* **35**: 1325-1332.

Hinton LK, Galetin A and Houston JB (2007) Multiple inhibition mechanisms and prediction of drug-drug interactions: comparison of metabolism and transporter models for predicting gemfibrozil-drug interactions. *Pharm Res* (In Press)

Hoffmaster KA and Brouwer K (2003) Impact of P-glycoprotein (P-gp) on the initial uptake of [D-penicillamine2,5]-enkephalin (DPDPE) in freshly isolated rat hepatocytes (Abstract). Poster presented at the AAPS Workshop on Drug Transport, Peach Tree City, GA, 10-12 February.

Houston JB and Carlile DJ (1997) Prediction of hepatic clearance from microsomes, hepatocytes, and liver slices. *Drug Metab Rev* **29**:891-922.

Jones HM, Nicholls G and Houston JB (2005) Impact of end-product inhibition on the determination of in vitro metabolic clearance. *Xenobiotica* **35**: 439-454.

Jones K, Bray PG, Khoo SH, Davey RA, Meaden ER, Ward SA and Back DJ (2001) P-Glycoprotein and transporter MRP1 reduce HIV protease inhibitor uptake in CD4 cells: potential for accelerated viral drug resistance? *AIDS* **15**:1353-1358.

Kashuba AD (2005) Drug-drug interactions and the pharmacotherapy of HIV infection. *Top HIV Med* **13**: 64-69.

Kim RB, Fromm MF, Wandel C, Leake B, Wood AJJ, Roden DM and Wilkinson GR (1998) The drug transporter P-glycoprotein limits oral absorption and brain entry of HIV-1 protease inhibitors. *J Clin Invest* **101**:289-294.

Khoo SH, Hoggard PG, Williams I, Meaden ER, Newton P, Wilkins EG, Smith A, Tjia JF, Lloyd J, Jones K, Beeching N, Carey P, Peters B and Back DJ (2002) Intracellular accumulation of human immunodeficiency virus protease inhibitors. *Antimicrob Agents Chemother* **46**: 3228-3235.

Koudriakova T, Iatsimirskaia E, Utkin I, Gangl E, Vouros P, Storozhuk E, Orza D, Marinina J and Gerber N (1998) Metabolism of the human immunodeficiency virus protease inhibitors indinavir and ritonavir by human intestinal microsomes and expressed cytochrome P4503A4/3A5: mechanism-based inactivation of cytochrome P4503A by ritonavir. *Drug Metab Dispos* **26**:552-561.

Kumar GN, Rodrigues DA, Buko AM and Denissen JF (1996) Cytochrome P450-mediated metabolism of the HIV-1 protease inhibitor ritonavir (ABT-538) in human liver microsomes. *J Pharm Exp Ther* **277**: 423-431.

Lam JL and Benet ZL (2004) Hepatic microsome studies are insufficient to characterise in vivo hepatic metabolic clearance and metabolic drug-drug interactions: studies of digoxin metabolism in primary rat hepatocytes versus microsomes. *Drug Metab Dispos* **32**: 1311-1316.

Lam JL, Okochi H, Huang Y and Benet LZ (2006) In vitro and in vivo correlation of hepatic transporter effects on erythromycin metabolism: characterising the importance of transporter-enzyme interplay. *Drug Metab Dispos* **34**: 1336-1344.

Lau YY, Okochi H, Huang Y and Benet LZ (2006) Multiple transporters affect the disposition of atorvastatin and its two active hydroxyl metabolites: application of *in vitro* and *ex situ* systems. *J Pharmacol Exp Ther* **316**: 762-771.

Lau YY, Sapidou E, Cui X, White RE and Cheng K-C (2002) Development of a novel *in vitro* model to predict hepatic clearance using fresh, cryopreserved and sandwich-cultured hepatocytes. *Drug Metab Dispos* **30**: 1446-1454.

Lin JH (1997) Human immunodeficiency virus protease inhibitors: From drug design to clinical studies. *Adv Drug Deliv Rev* **27**:215-233.

McGinnity DF, Soars MG, Urbanowiz RA and Riley RJ (2004) Evaluation of fresh and cryopreserved hepatocytes as in vitro drug metabolism tools for the prediction of metabolic clearance. *Drug Metab Dispos* **32**: 1247-1253.

McNicholl IR (2004) Drug interactions among the antiretrovirals. *Curr Infec Dis Rep* **6**:159-162.

McRae MP, Lowe CM, Tian X, Bourdet DL, Ho RH, Leake BF, Kim RB, Brouwer KLR and Kashuba ADM (2006) Ritonavir, saquinavir and efavirenz but not nevirapine, inhibit bile acid transport in human and rat hepatocytes. *J Pharmacol Exp Ther* **318**:1068-1075.

Mizuno N, Niwa T, Yotsumoto Y and Sugiyama Y (2003) Impact of drug transporter studies on drug discovery and development. *Pharmacol Rev* **55**:425-61.

Muck W, Mai I, Fritsche L, Ochmann K, Rohde G, Unger S, Johne A, Bauer S, Budde K, Roots I, Neumayer HH and Kuhlmann J (1999) Increase in cerivastatin systemic exposure after single and multiple dosing in cyclosporine-treated kidney transplant recipients. *Clin Pharmacol Ther* **65**:251-261.

Obach RS (2001). The prediction of human clearance from hepatic microsomal data. *Curr Opin Drug Discov Dev* **4**: 36-44.

Rawden HC, Carlile DJ, Tindall A, Hallifax D, Galetin A, Ito K and Houston JB (2005) Microsomal prediction of in vivo clearance and associated inter individual variability of six benzodiazepines in humans. *Xenobiotica* **35**: 603-625.

Shibata N, Gao W, Okamoto H, Kishida T, Iwasaki K, Yoshikawa Y and Takada K (2002a) Drug interactions between HIV protease inhibitors based on physiologically-based pharmacokinetic model. *J Pharm Sci* **91**:680-689.

Shibata N, Gao W, Okamoto H, Kishida T, Yoshikawa Y and Takada K (2002b) In-vitro and in-vivo pharmacokinetic interactions of amprenavir, an HIV protease inhibitor, with other current HIV protease inhibitors in rats. *J Pharm Pharmacol* **54**:221-229.

Shitara Y, Itoh T, Sato H, Li AP and Sugiyama Y (2003) Inhibition of transporter-mediated hepatic uptake as a mechanism for drug-drug interaction between cerivastatin and cyclosporin A. *J Pharmacol Exp Ther* **304**:610-616.

Shitara Y, Horie T and Sugiyama Y (2006) Transporters as a determinant of drug clearance and tissue distribution. *Eur J Pharm Sci* **27**:425-446.

Srinivas RV, Middlemas D, Flynn P and Fridland A (1998) Human immunodeficiency virus protease inhibitors serve as substrates for multidrug transporter proteins MDR1 and MRP1 but retain antiviral efficacy in cell lines expressing these transporters. *Antimicrob Agents Chemother* **42**:3157-3162.

Su Y, Zhang X and Sinko PJ (2004) Human organic anion-transporting polypeptide OATP-A (SLC21A3) acts in concert with P-glycoprotein and multidrug resistance protein 2 in the vectorial transport of saquinavir in Hep G2 cells. *Mol Pharm* **1**:49-56.

Tirona RG, Leake BF, Wolkoff AW and Kim RB (2003) Human organic anion transporting polypeptide-C (SLC21A6) is a major determinant of rifampin-mediated pregnane X receptor activation. *J Pharmacol Exp Ther* **304**:223-228.

Yamaji H, Matsumura Y, Yoshikawa Y and Takada K (1999) Pharmacokinetic interactions between HIV-protease inhibitors in rats. *Biopharm Drug Dispos* **20**:241-247.

Zamek-Gliszczynski MJ, Hoffmaster KA, Nezasa K, Tallman MN and Brouwer KLR (2006) Integration of hepatic drug transporters and phase II metabolising enzymes: Mechanisms of hepatic excretion of sulphate, glucuronide and glutathione metabolites. *Eur J Pharm Sci* **27**: 447-486.

Zhang KE, Wu E, Patick AK, Kerr B, Zorbas M, Lankford A, Kobayashi T, Maeda Y, Shetty B and Webber S (2001) Circulating metabolites of the human immunodeficiency virus protease inhibitor nelfinavir in humans: structural identification, levels in plasma, and antiviral activities. *Antimicrob Agents Chemother* **45**:1086-1093.

**FOOTNOTE**

AJP was financially supported by a BBSRC CASE studentship with Roche Products Limited.

**Figure Legends**

**Figure 1**

Relationship between rate of metabolism and substrate concentration for saquinavir in suspended rat hepatocytes (A) and rat liver microsomes (B), (mean of 3 preparations). Corresponding clearance plots for saquinavir in rat hepatocytes (C) and rat liver microsomes (D).

**Figure 2**

Clearance plot showing substrate concentration dependence for nelfinavir in rat liver microsomes (A) and suspended rat hepatocytes (B) (mean of 3 preparations)

**Figure 3**

Clearance plot for ritonavir in rat liver microsomes (A) and suspended rat hepatocytes (B) (mean of 3 preparations)

**Figure 4**

Typical plot showing initial formation rate of ritonavir metabolites M1 (○), M2 (△), M9 (□) and M11 (◇) with respect to ritonavir concentration in suspended rat hepatocytes (A) and microsomes (B).

**Figure 5**

Uptake rates over a substrate concentration range for saquinavir (A), nelfinavir (B) and ritonavir (C) into rat hepatocytes at 37ºC (▼) and 4ºC (▽) and the difference in rates (closed

symbols), (mean of 3 preparations for saquinavir and nelfinavir, mean of 2 preparations for ritonavir). Panel 5D shows the time course for uptake of saquinavir (◆), nelfinavir (■) and ritonavir (●) (5 μM) over 2 min in rat hepatocytes at 37ºC (mean of 2 preparations ).

**Figure 6**

Relationship between saquinavir (I), nelfinavir (II) and ritonavir (III) metabolism in rat liver microsomes (◇, □ and ○ respectively), suspended rat hepatocytes (◆, ■ and ● respectively) and uptake in suspended rat hepatocytes (▲). Panels A and B show mean rates and clearance (n=3), respectively as a function of substrate concentration.

Table 1: Non-specific binding characteristics of saquinavir, ritonavir and nelfinavir

| | **fu in incubation matrix** | | | **% loss due to non-specific binding** | |
|---|---|---|---|---|---|
| | Hepatocyte metabolism buffer (0.2% BSA) | Microsomes (0.2 mg protein/ml) | Hepatocyte uptake buffer (2% BSA) | Microsomes (0.2 mg protein/ml) | Hepatocyte (0.02% BSA, 0.2 x$10^6$ cells/ml) |
| Saquinavir | 0.33 | 0.34 | 0.15 | 16% | 52% |
| Ritonavir | 0.5 | 0.6 | 0.12 | 14% | 39% |
| Nelfinavir | 0.52 | 0.10 | 0.08 | 26% | 44% |

Table 2: Hepatocyte kinetic parameters for uptake and metabolism of saquinavir, ritonavir and nelfinavir (n=3)

| | Metabolism Parameters | | | Uptake Parameters | | |
|---|---|---|---|---|---|---|
| | $K_m$ (µM) | $V_{max}$ (pmol/min/$10^6$ cells) | $Cl_{int}$ (µl/min/$10^6$ cells) | $K_m$ (µM) | $V_{max}$ (nmol/min/$10^6$ cells | Perm (µl /min/$10^6$ cells |
| Saquinavir | 0.27 ± 0.15 | 114 ± 62.5 | 486 ± 256 | >28 | >18 | 520 |
| Ritonavir | 0.034 ± 0.013 | 21.6 ± 6.18 | 734 ± 384 | 14 ± 5.4 | 15 ± 6 | 1070 |
| Nelfinavir | 0.21 ± 0.12 | 232 ± 50.2 | 1290 ± 464 | 22.4 ± 5 | 58.4 ± 17.8 | 2670 |

Mean ± sd of triplicate in vitro preparations

Table 3: Kinetic parameters of saquinavir, ritonavir and nelfinavir in rat liver microsomes (n=3)

| | $K_m$ (μM) | $V_{max}$ (pmol/min/mg protein) | $Cl_{int}$ (ml/min/mg protein) |
|---|---|---|---|
| Saquinavir | 0.042 ± 0.05 | 446 ± 89 | 11 ± 7 |
| Ritonavir | 0.0055 ± 0.0041 | 53.3 ± 16.5 | 11.9 ± 4.4 |
| Nelfinavir[a] | 0.007 ± 0.002 (*0.01*) | 100 ± 9.7 (*120*) | 15.7 ± 5.4 (*11.4*) |

Mean ± sd of triplicate in vitro preparations

[a]values in parenthesis denote parameters estimated from a substrate inhibition fit

DMD Fast Forward. Published on April 21, 2008 as DOI: 10.1124/dmd.108.020917
This article has not been copyedited and formatted. The final version may differ from this version.



Table 4: Hepatocyte: medium concentration ratios for total ($K_p$) and unbound ($K_{pu}$) and intracellular fraction unbound for saquinavir, nelfinavir and ritonavir

| | $K_p$ | $K_{pu}$ | Intracellular fraction unbound |
|---|---|---|---|
| Saquinavir | 306 | 6.8 | 0.022 |
| Ritonavir | 616 | 11.4 | 0.018 |
| Nelfinavir | 3352 | 5.7 | 0.0017 |

Mean of duplicate determinations

DMD Fast Forward. Published on April 21, 2008 as DOI: 10.1124/dmd.108.020917
This article has not been copyedited and formatted. The final version may differ from this version.



Table 5: Comparison of predicted metabolic clearance and permeability parameters from hepatic microsomes and hepatocytes, expressed per unit weight of liver and hepatic extraction ratios reported in vivo and predicted from the vitro systems

| | Microsomal Clearance (ml/min/g liver)[a] | Predicted Extraction ratio from microsomes[b] | Hepatocytes Permeability (ml/min/g liver)[a] | Predicted Extraction ratio from hepatocytes[b] | Hepatocytes Clearance (ml/min/g liver)[a] |
|---|---|---|---|---|---|
| Saquinavir | 650 | 0.95 | 57 | 0.67 | 53 |
| Ritonavir | 714 | 0.96 | 117 | 0.81 | 80 |
| Nelfinavir | 940 | 0.96 | 284 | 0.87 | 141 |

[a] Scaled to whole liver with scaling factors listed in Methods

[b] Calculated from the well-stirred liver model with fu in blood from Shibata et al., 2002a and a hepatic blood flow of 100ml/min/kg

**Fig 1**

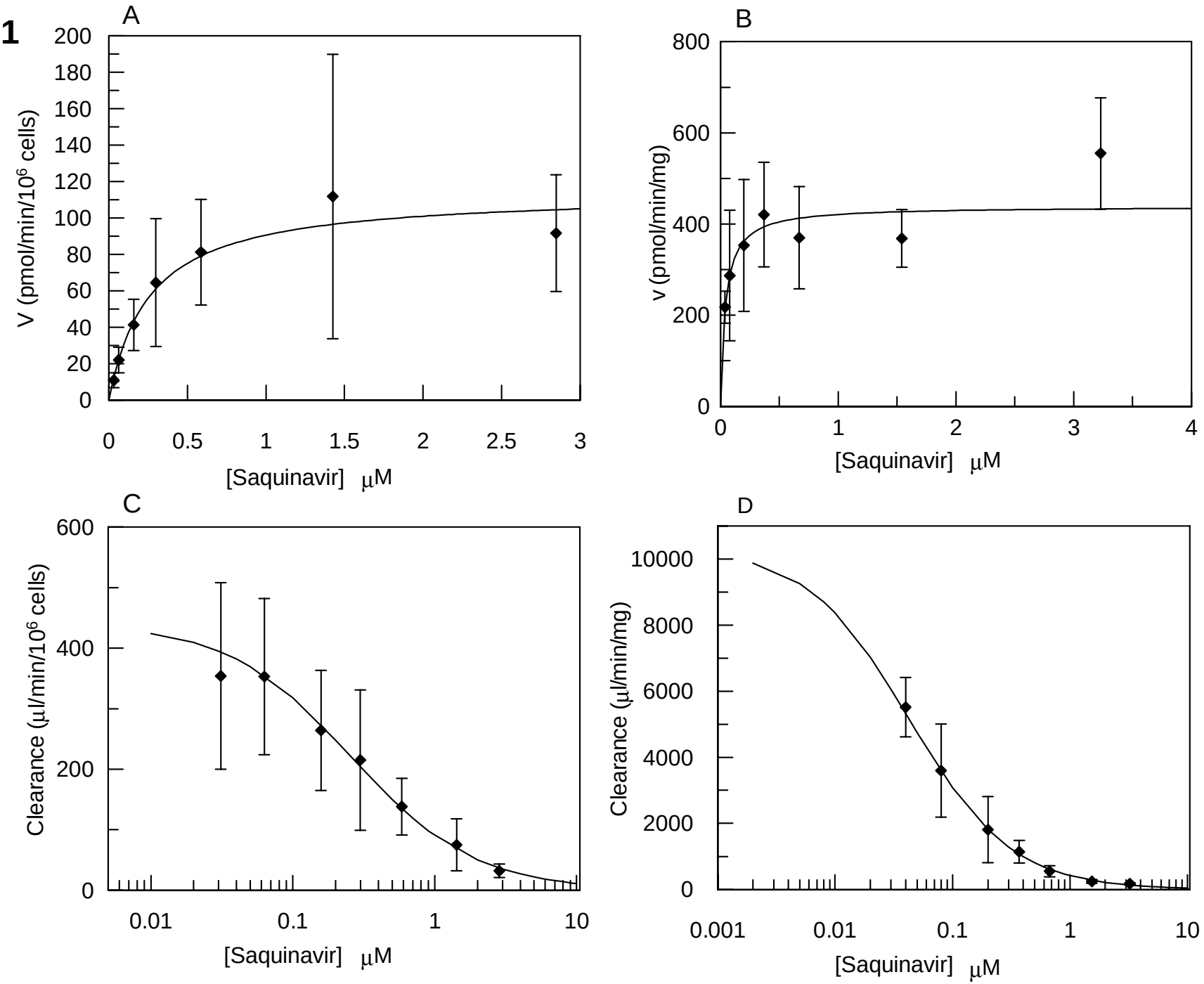

# Fig 2

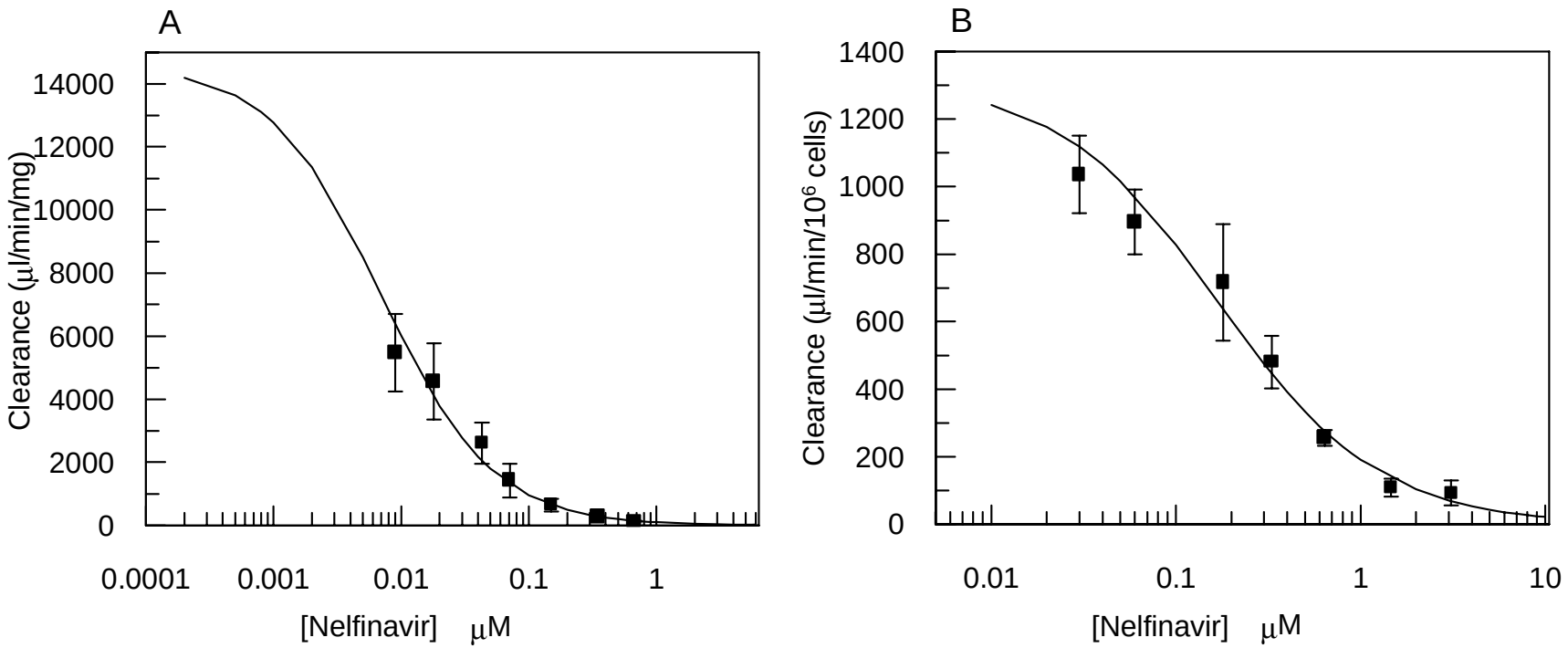

# Fig 3

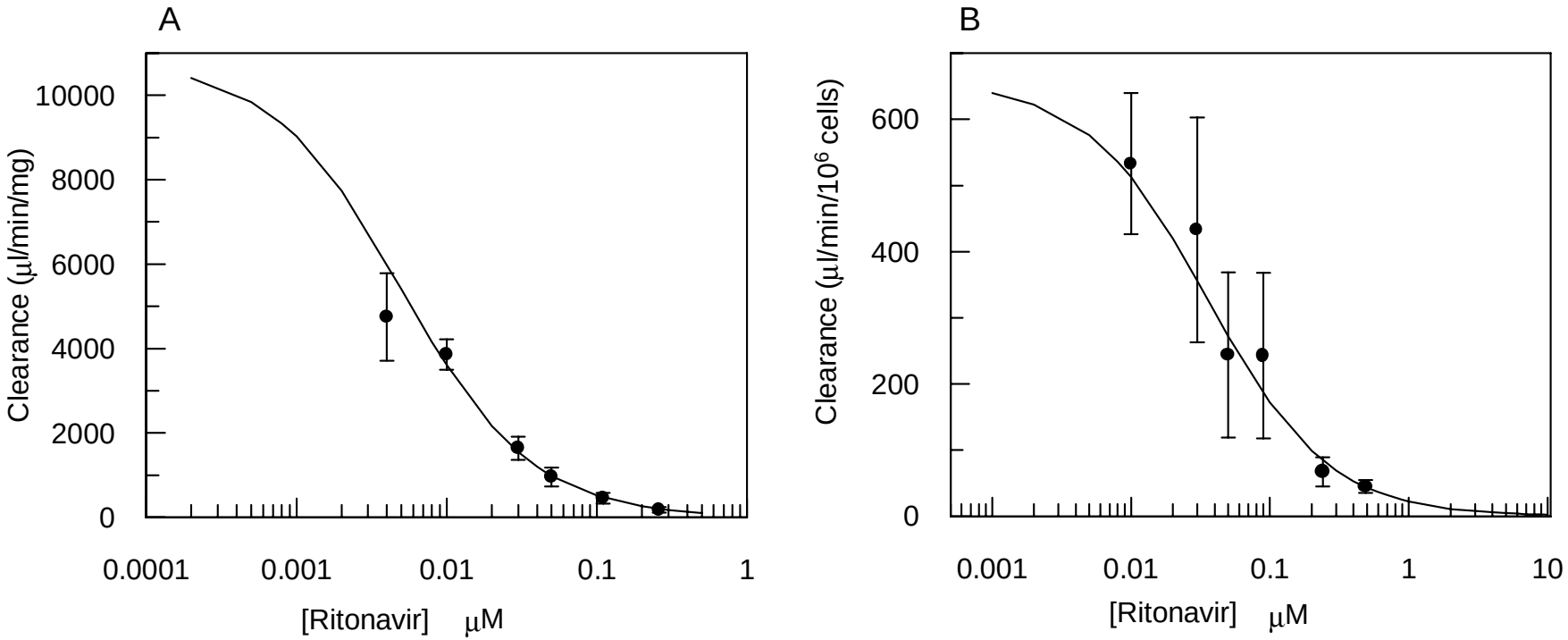

# Fig 4

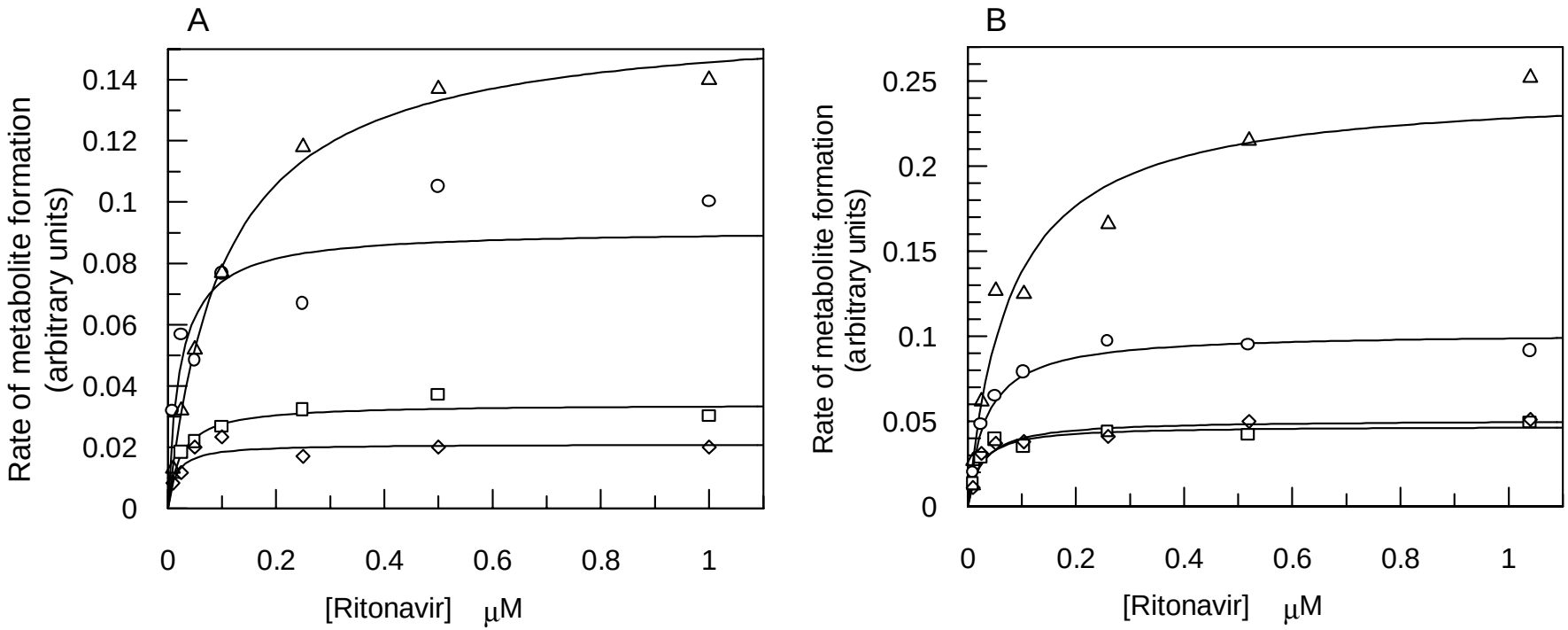

# Fig 5

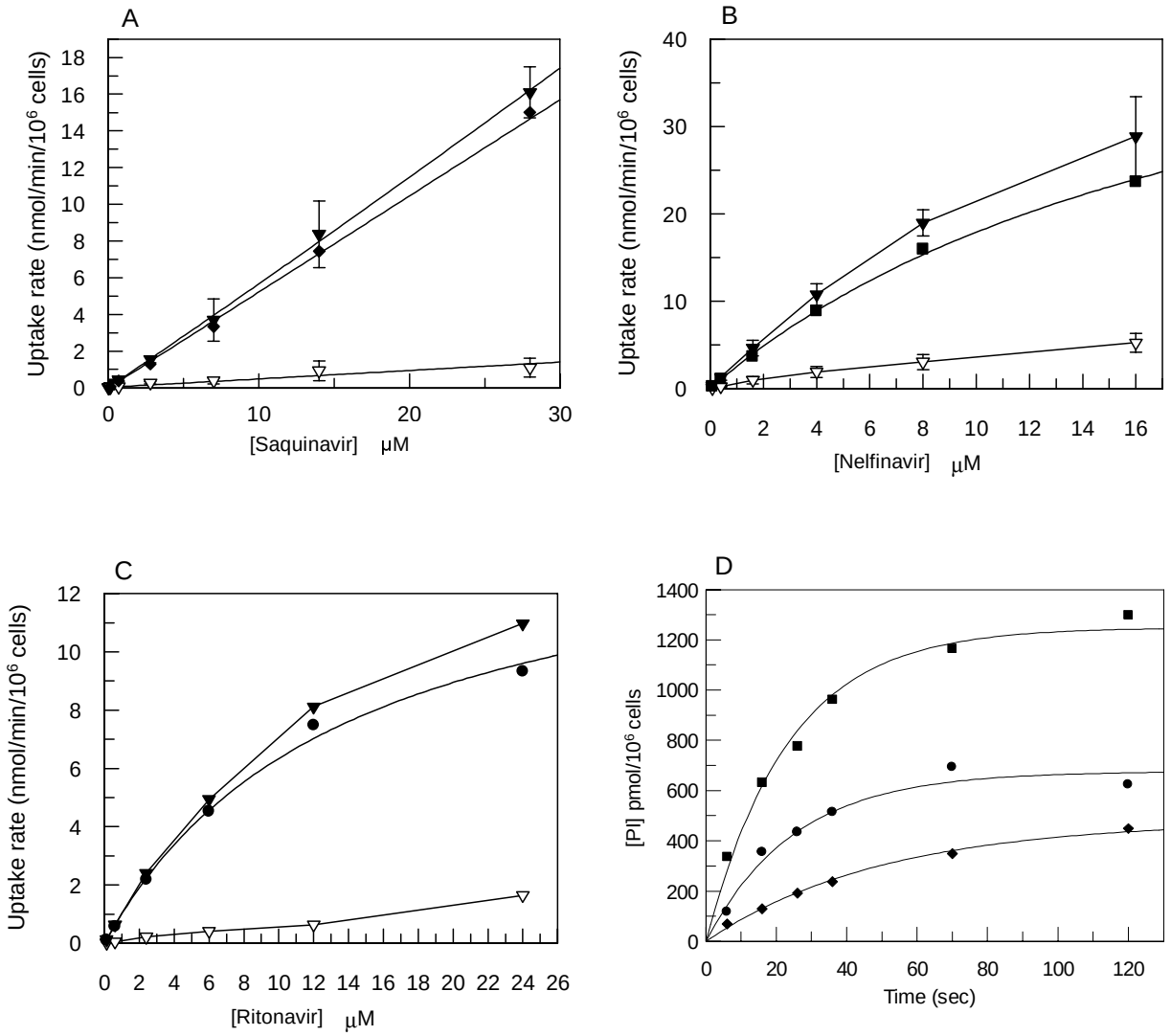

# Fig 6